Adv Polym Sci (2006) 200: 71–90
DOI 10.1007/12_006

Published online: 28 October 2005

Liquid Crystallinity in Block Copolymer Films for Controlling Polymeric Nanopatterns

Wim H. de Jeu (✉) · Yaëlle Séréro · Mahmoud Al-Hussein

FOM-Institute for Atomic and Molecular Physics (AMOLF), Kruislaan 407, 1098SJ Amsterdam, The Netherlands
dejeu@amolf.nl

Abstract We review thin-film morphologies of hybrid liquid-crystalline/amorphous block copolymers. The microphase separation of the blocks and the smectic liquid crystalline ordering within one of the blocks are treated systematically in terms of the interaction parameters. The competition of the "tandem" interactions in terms of length scales and of surface anchoring can be used advantageously to control the orientation of block interfaces for nanopatterning.

Keywords Block copolymers · Nanostructures · Smectic liquid crystals · Thin films

Abbreviations

AFM	atomic force microscopy
GIXD	grazing-incidence X-ray diffraction
GISAXS	grazing-incidence small-angle X-ray diffraction
LC	liquid crystal(line)
ODT	order-disorder transition
XR	X-ray reflectivity

1 Introduction

Several future technologies demand structures at length-scales below 1 μm (say 1–100 nm). In various cases such structures have to be ordered in a regu-

lar and tuneable fashion while in addition specific physical properties are needed. These requirements can often be met using the surfaces of polymers. Structural order over many length scales can be created by self-organizing polymer materials, controlled and possibly directed by molecular interactions and external constraints. Self-organization occurs from nanoscopic to macroscopic scales and includes phenomena like phase separation or microphase separation, adsorption and crystallization. Apart from potential applications, they are important for fundamental studies investigating the relation between nanostructure and resulting physical properties. In spite of considerable effort in this field, it is difficult to orient or align polymeric nanostructures. Thus, a major goal of present research is to arrange the polymeric features in regular well-ordered arrangements exhibiting multiple length scales [1]. Several competing factors are able to control the structure formation (chemical differences, conformational entropy, spatial constraints, external fields).

In this chapter we concentrate on block copolymers, which are well known to microphase separate in various structures that are scientifically interesting as well as technologically attractive [2, 3]. In thin films these structures can be further influenced by specific interactions between the various blocks and the limiting interfaces. However, in the context of nano-ordering, these possibilities of forming fairly well-defined mesoscopic structures are not sufficient. To obtain control over the ordering process, further handles are needed which can be provided by additional ordering principles in one of the blocks. Though again several mechanisms exist, we shall discuss here the possibilities of liquid crystalline (LC) ordering in one of the blocks, in particular smectic LC ordering. We restrict ourselves also to simple substrates, and refrain from the interesting field of "replication" of patterned surfaces, see for example [4–6].

In the next section the basic properties of block copolymers and liquid crystalline polymers will be summarized. Furthermore, we discuss the block microphase separation and its interaction with the LC ordering in one of the blocks in a systematic way. In the remaining sections a couple of examples (see Table 1) will be discussed of competing hierarchical ordering at surfaces, with emphasis on the possibilities for controlled nanopatterning.

Table 1 Compounds discussed and their properties

Polymer	M_n	$\Phi_{LC\text{-block}}$	DP	Phase behavior (°C)	Refs.
PS-*b*-PChEMA	57 000	0.51	1.1	g_{PS} 101 g_{PChEMA} 126 Sm-A 187 I	[43, 44]
PIBVE-*b*-PLC	9600	0.67	1.26	g_{PIBVE} −19 g_{LC} 11 Sm-C* 44 Sm-A 67 I	[47, 48]
PMMA-*b*-PF8H2A	45 400	0.79	1.2	Sm-A 85 I	[54, 55]

2 Liquid Crystalline/Amorphous Block Copolymers

The simplest case of a block copolymer is a diblock consisting of two covalently bonded polymers with chemically distinct repeat units A and B. If A and B are incompatible, below the order-disorder transition at T_{ODT} microphase separation is obtained into, for example, a spherical, cylindrical, or lamellar phase. The phase behavior depends on the relative volume fraction of A and B and on the magnitude of the product $\chi_{AB}N$, where χ_{AB} is the Flory–Huggins interaction parameter between the two polymers, and N the total degree of polymerization [7]. We can write

$$\chi_{AB} = \frac{Z}{k_B T}\left[\varepsilon_{AB} - \frac{1}{2}(\varepsilon_{AA} + \varepsilon_{BB})\right], \tag{1}$$

in which ε is the interaction energy and Z the number of nearest-neighbor contacts. Note that $\chi \sim 1/T$. In the case of roughly equal block sizes, the block copolymer microphase separates into a lamellar phase, the scaling of the lamellar period being $\sim N^{2/3}$. This result stems from the balance between the enthalpy gain of demixing A and B (Eq. 1) and the entropy cost of chain confinement within the layers [7–9]. For increasingly asymmetric volume fractions the lamellar structure makes way successively for a hexagonal cylindrical and a spherical micellar structure, very similar to that observed for low-mass surfactants. In fact the situation is somewhat more complicated due to the possible interference of intermediate morphologies like a cubic gyroid phase and a perforated lamellar phase.

In thin films of diblock copolymers, the interactions occurring at the air/film and film/substrate interfaces influence the microphase separation process, and can be used to control the orientation of the morphology. For example, a preferential interaction of one of the blocks with the boundaries ("surfactant"-like behavior) will favor uniformity of a lamellar phase on a macroscopic scale, with the lamellae of periodicity L parallel to the substrate [10, 11]. The resulting film thickness will belong to a discrete spectrum of allowed values D_n, depending on the boundary conditions [10, 12] given by

$$D_n = (n + \frac{1}{2})L \quad \text{or} \quad D_n = nL\,. \tag{2}$$

In the case where the actual thickness does not match this condition, terraces are formed with a height difference corresponding to L [13]. In a similar way the presence of interfaces will lead in other microphase-separated morphologies to some ordering of the cylinders or spheres. Note that structures of lamellae parallel to a substrate or cylinders perpendicular to a substrate are uniquely defined. However, this is no longer true when the lamellae are perpendicular or the cylinders parallel to the substrate. In the latter cases control of the azimuthal ordering in the plane of the film is needed to obtain uni-

form patterns. This is a crucial problem for the possible exploitation of such structures.

A combination of LC ordering and macromolecular properties can be obtained on a macroscopic scale in LC polymers [14, 15]. LC or mesogenic units can be built into a polymer in two different ways: as side groups attached to the polymer backbone (side-chain LC polymers) or built into the polymer backbone itself (main-chain LC polymers). The last class of materials can give strong fibbers, being best known under their trade names (Kevlar, Twaron). Side-chain LC polymers usually have an end group of the mesogenic units attached to the polymeric backbone via a flexible group that acts as a spacer. The resulting comb-shaped LC polymers are used as materials for the second-harmonic generation but also as protective coatings. Various types of LC phase (nematic, smectic) can be found, just as in the corresponding monomers, though in general the transition temperatures are shifted and the mesophases tend to be higher ordered than in the corresponding monomer systems. A special type of side-chain LC polymer is obtained if the mesogenic group is attached laterally to the polymer. In the absence of a spacer group this leads to stretching of the backbone into a rod-like shape: mesogenic jacketed LC polymers [16–18]. In this review we restrict ourselves to conventional comb-shaped LC polymers.

In the case of smectic-A (Sm-A) ordering the LC phase consists of stacks of liquid layers. In the context of nanostructuring this is the most relevant situation. The layer periodicity d can be close to the length of the side group (single layer), somewhat larger (interdigitation of the mesogenic groups) or about twice that value (double layers). The actual situation depends on the effective transverse dimension of the side group in relation to the spacing between the "anchoring" points at the polymeric backbone. In analogy to lamellar diblock microphase separation, the smectic ordering of a comb-shaped LC polymer can be considered as "nanophase" separation: the polymeric backbone separates from the mesogenic units [19, 20]. This analogy was nicely illustrated by Diele [20], who studied the smectic periodicity as a function of the number of side groups. Upon decreasing the density of attached side groups the smectic periodicity was found to increase. This can be understood if the mesogenic units always form the same type of smectic layering, forcing the backbone polymer to coil in between the layers (see Fig. 1a). With decreasing number of side groups, more backbone must be packed into this polymer sheet and its thickness increases. As a consequence also the smectic periodicity increases. One can push the analogy further by attributing an effective χ-parameter to the interaction backbone-mesogens. The situation mentioned then corresponds to strong phase separation; in other cases (weak phase separation) the backbone might be less strictly confined between the mesogenic layers. The Sm-A-nematic (T_{AN}) or smectic-isotropic (T_{Ai}) phase transition temperature can be considered as the relevant T_{ODT}.

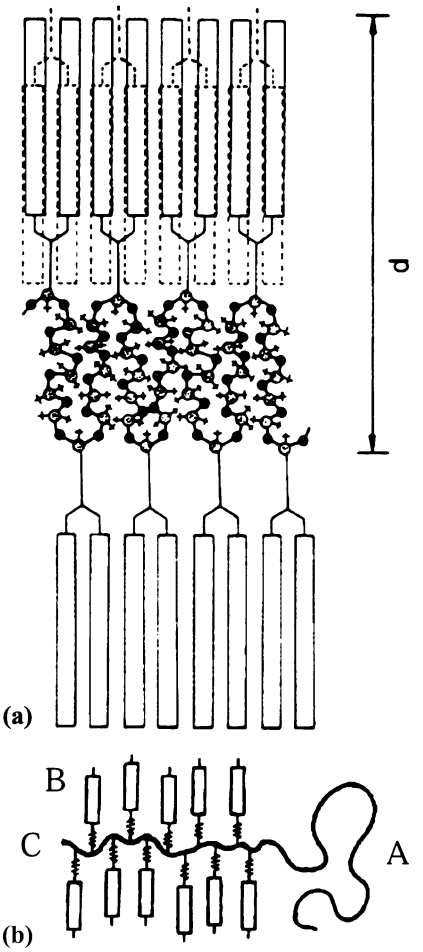

Fig. 1 **a** Smectic LC ordering as a nanophase separation process. The picture shows smectic layering when for only one out of five backbone positions a side chain is attached [20]. **b** Cartoon model of a LC/amorphous diblock copolymer

In hybrid amorphous/smectic block copolymers a hierarchical interplay arises between block copolymer ordering on the scale of tens of nm and smectic layering on the scale of nm. In addition to the enthalpy gain of demixing A and B and the entropy cost of chain stretching involved in "classical" microphase separation, several additional contributions to the free energy of block copolymers come into play. These include (i) the elastic energy of the LC phase and (ii) the orientational wetting of the LC phase at the internal micro-domain boundaries as well as (iii) at the external film surfaces. For strong block segregation the LC phase is confined by the amorphous block, similar to crystallization of block copolymers with a semi-crystalline block.

For weak block segregation the coupling may be more important and T_{AN} or T_{Ai} may act also as T_{ODT} for the block separation. On the other hand the LC phase behavior may be influenced by the confinement. In particular if the LC phase is the minority phase, in the case of spherical or cylindrical morphologies smectic ordering may be suppressed and nematic ordering favored. For lamellar block copolymer morphologies the smectic layers are usually oriented perpendicular to the block interfaces. The influence of molecular mass and polydispersity has hardly been investigated yet [21]. Some reviews in the field of LC/amorphous block copolymers are given in [22–26], a selection of original papers in [27–36].

In the spirit of the discussion so far, an amorphous/smectic LC diblock can be considered to be an A(CB) triblock copolymer, where A denotes the amorphous polymer and C and B the backbone and mesogens of the smectic polymer, respectively (Fig. 1b). If $T_{Ai} \ll T_{ODT}$, the Sm-A phase forms within a well microphase-separated block system and one would expect $\chi_{BC} \ll \chi_{AC}, \chi_{AB}$. Only when this condition is fulfilled the usual description as a diblock system is effectively correct. However, a different situation arises if the backbone in the smectic polymer is similar to the polymer in the amorphous block: $C \equiv A' \approx A$. Now little incompatibility exists between the polymer in the amorphous block and the backbone of the smectic LC block. In that situation $\chi_{AC} \approx 0$, and $\chi_{BC} \approx \chi_{AB} \gg 0$. A correct description of this situation would be A(A′B), and the interplay between the smectic ordering and the microphase separation is expected to become more important.

The competing hierarchical ordering in amorphous/smectic block copolymers provides a new handle to manipulate the structure in thin films. Let us consider as an example lamellar block structures. In bulk the smectic layers are usually orthogonal to the lamellae and separate the microphase segregated blocks. This can be understood from minimum contact interactions between the two polymer chains. As discussed above, in thin films the block lamellae in general like their interfaces to be parallel to the substrate. However, in such films the mesogenic units in a side-chain LC polymer prefer usually homeotropic anchoring to both the substrate and the air interface [37] (except for strongly polar end groups). For a smectic LC phase this would bring the smectic layers also parallel to the substrate. In that case a conflict arises between the directions of the smectic layering and the block lamellar ordering, that cannot both adjust to the same preferred boundary orientation and remain orthogonal to each other. The resulting frustration can be used advantageously for control purposes. In principle the film should be annealed at temperatures within the range of stability of the smectic phase. This requires T_{AN} or T_{Ai} to be larger than any glass transition in the system. Annealing at high temperatures well below T_{ODT} but above T_{AN} or T_{Ai} and subsequent cooling into the smectic phase is less suitable as it decouples the formation of the smectic layering from the initial block organization. Nevertheless, in such a situation smectic layering can already exist locally at the film interfaces.

In the following sections we shall illustrate these concepts by means of a few different examples. Similar considerations apply to the work of Ikkala and co-workers, who investigated systems with amphiphilic molecules attached via hydrogen bonding to one block of a diblock copolymer [38, 39]. In that situation the temperature at which the hydrogen bonding gets lost (around 80 °C) sets a limit to interactive annealing. The combination of X-ray reflectivity (XR) and atomic force microscopy (AFM) has proven to be most useful in gaining access to complementary real-space information of the surface and reciprocal-space knowledge of the interior of the films. As XR is sensitive to modulations of the average electron density along the surface normal [40], in this way a complete model of the thin film structure can be obtained, including possible differences between the surface and the interior of the film. Similar arguments apply to any lateral ordering of the film. Complementary to surface ordering probed by AFM, grazing-incidence X-ray diffraction (GIXD [41], including GISAXS at small azimuthal angles [42], can tell whether this ordering is continued through the whole film.

3 Example 1. Smectic/Amorphous AB Diblock Copolymer

In this first example, we investigate the lamellar thin film morphology of the approximately symmetric amorphous-smectic diblock copolymer PS-*b*-PChEMA. The molecular structure is shown in Fig. 2a while further molecular and phase information is given in Table 1. In the bulk the smectic layers ($d = 4.3$ nm) and the block lamellae ($L = 30$ nm) are orthogonal as anticipated [43]. Spin-coated films were annealed in the smectic phase around 170 °C, well above the glass transition of PS. XR measurements for films of different thickness D are displayed in Fig. 2b. A developing quasi-Bragg peak can be observed in thin films, with an associated periodicity of 4.2 nm that corresponds closely to the bulk smectic spacing of PChEMA. However, this observation is restricted to thin films with approximately $D \leq 2L$; for thicker films the situation is less clear. Thin films were investigated in some detail by Wong et al. [44]. The smectic layers are parallel to the surface, with the mesogenic side groups anchoring homeotropically, perpendicular to the surface. The same homeotropic anchoring is observed in XR measurements of PChEMA homopolymer thin films. The surface topography of a typical sample prepared under the same conditions and measured with AFM is given in Fig. 3a. The average thickness as measured is 33 nm, and two types of terrace with an average height difference of 5 nm can be seen. The latter value is comparable to the thickness of a smectic layer. This is consistent with the previous X-ray observation, and confirms that the smectic layers formed from the mesogenic side groups are parallel to the surface. In adjusting the thickness D to the boundary conditions, an integral number of smectic layers $D = nd$ now

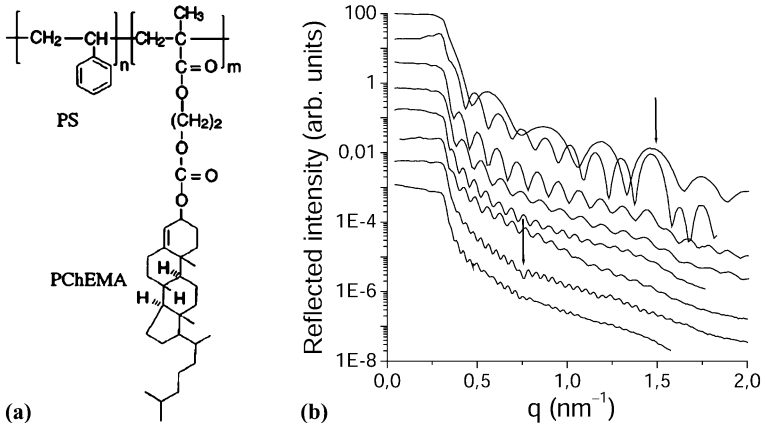

Fig. 2 **a** Structure of PS-*b*-PChEMA. **b** XR of films of various thickness, from *top* to *bottom*: 22, 45, 53.5, 55.5, 88, 91.5, 138, and 152 nm, respectively. The *upper arrow* indicates for thin films smectic layering parallel to the substrate; the *lower arrow* for thick films (weak) lamellar block orientation parallel to the substrate

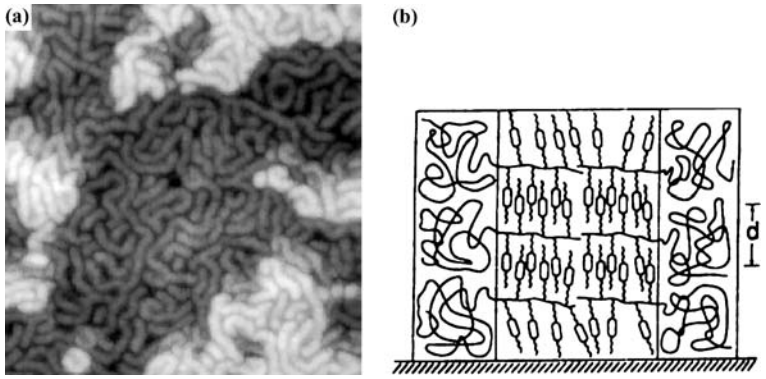

Fig. 3 **a** Perpendicular lamellae for a 36 nm thick PS-*b*-PChEMA film as observed by AFM ($1 \times 1\ \mu m^2$ viewing area). **b** Schematic representation of the perpendicular wetting [44]

takes the place of the quantization in L given by Eq. 2. The serpentine corrugations on the terraces in Fig. 3a have an average in-plane spatial period of 32 ± 4 nm, which is essentially the ABBA lamellar period.

The combination of XR and AFM results indicates that the generic ordering found in isotropic symmetric diblock films, where the lamellae are parallel to the surface, has been suppressed in these thin hybrid diblock films (Fig. 3b). The anchoring of the mesogenic groups dominates the wetting, and the hybrid diblock lamellae order in a direction perpendicular to the surface. PChEMA readily wets both the quartz and air interfaces and PS is usually repelled from hydrophilic substrates. Hence, intuition informed

by theoretical descriptions of isotropic diblocks suggests that the contact interaction should dominate and lead to parallel wetting of the lamellae, with homeotropic PChEMA at both interfaces. For PS-*b*-PChEMA, however, homeotropic anchoring of the PChEMA side groups is inherently antagonistic to parallel wetting, because it necessarily generates defects and extra unfavorable segment-segment contact near PS-PChEMA interfaces. More important, the equilibrium bulk lamellar period defines a thickness for the PChEMA block at the interface, which is in general not commensurate with the thickness of an integral number of homeotropic smectic layers. This incommensurability is particularly strong for thin films in which D and L are of the same order but not equal. The frustration from both effects, however, can be avoided in perpendicular wetting of the lamellae, for which homeotropic anchoring is maintained without layer incommensurability, but at the cost of some unfavorable PS wetting at the substrate. The parallel ordering of lamellae, however, can be restored in asymmetric lamellar diblocks in which the contact area between PS and the substrate is increased [44]. In thicker films possibly a transition takes place from perpendicular lamellae at the substrate to parallel lamellae at the air interface, attributed to a decreased incommensurability. However, this point has not been investigated more extensively.

In spite of the interesting perpendicular morphology in thin films, the azimuthally random serpentine-like nature of the block lamellae prevents useful applications. Two possibilities have been explored to modify locally the substrate in order to create a preferential in-plane anchoring direction. The first is to play with the topography of the substrate. A sharp step on a silicon wafer will select a particular direction that may influence the orientation of the structure. Preliminary results for a film deposited on a saw-tooth patterned silicon wafer lead indeed to lamellae oriented in the step direction (see Fig. 4a). A second option consists of modifying on a nanometer scale the affinity of the substrate for the blocks. It is possible to graft alkyl chains on a silicon surface at selected positions determined by scratching the substrate in the presence of an appropriate solution of the grafting molecules [45]. Performing this scratching with an AFM cantilever tip, one can create a well-defined hydrophobic nanoline on the hydrophilic surface. As PS is a nonpolar polymer, it will preferably wet such a line. As shown in Fig. 4b this induces indeed some ordering of the lamellar features. However, in both cases the correlation lengths of the parallel oriented lamella is limited. In combination with the rather elaborate methods of obtaining the alignment, this is so far prohibitive for further applications.

In conclusion we have reached a morphology of stable lamellae oriented perpendicular to a nontreated substrate. Similar results have recently been reported by Hashimoto and co-workers using conventional lamellar block copolymers on a strongly corrugated substrate [46]. In both situations azimuthal ordering of the lamellae turned out to be difficult. We wanted to extend these experiments to a cylindrical morphology for which we should

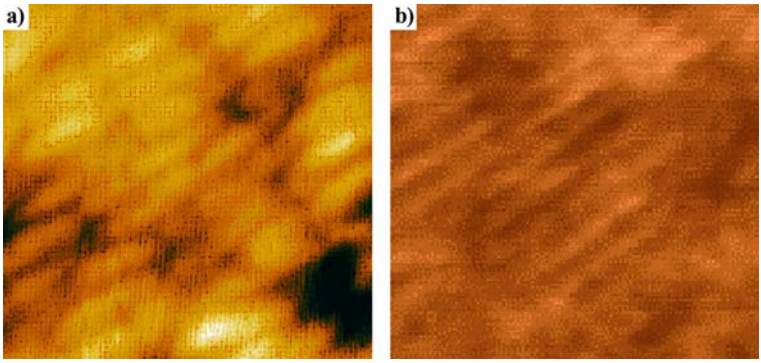

Fig. 4 AFM image of the alignment of perpendicular lamellae of a thin PS-*b*-PChEMA film along **a** a grating and **b** near a locally functionalized nano-scratch (see text, $0.35 \times 0.35\ \mu m^2$)

expect the smectic layers to stabilize in thin film cylinders perpendicular to the substrate. However, though the analogous compound PS-*b*-PChEMA with 30–40% PS gives a cylindrical morphology, somewhat unexpectedly the smectic layers orient parallel to the block interfaces (cylinder axes) [43]. We attribute this anomalous behavior to the relatively low molecular mass of the particular block copolymers. Anyhow, it removed our "control handle" and made us turn to other systems (see Sect. 5).

4 Example 2. Smectic/Amorphous A(A′B) "Triblock" Copolymer

The next example consists of an amorphous polymer, which consists of a poly(isobutylvinylether) (PIBVE), chemically linked to a side-chain LC block with as a backbone the same vinyl ether. The structure is shown in Fig. 5a and further information is presented in Table 1. Note that the Sm-A phase region is at relatively low temperatures. Annealing was done close to T_{Ai}, subsequently the sample was quenched to room temperature for further analysis. As the amorphous block is only incompatible with the side-chain part of the LC block we expect the LC properties to be dominant. The system falls in the triblock class A(A′B) as described in Sect. 2. Nevertheless, two glass transitions have been detected in DSC, which is a direct proof of the immiscibility of the two blocks [47]. Films of the LC homopolymer indicate smectic layers parallel to the substrate with a periodicity of $d = 3.1$ nm. The period is equal to the stretched size of the side groups, which are homeotropically oriented. This leads to a model of interdigitated side groups. A sample annealed in the isotropic phase indicates preferential interactions between the boundary layer and the substrate. XR shows that the film starts dewetting

from the substrate except for a layer of 6.2 nm, corresponding to exactly two smectic layers.

The XR curve from a diblock film is given in Fig. 5b [48]. In addition to the Kiessig fringes several additional periodicities show up. Bragg-like features at $q_z \approx 7\ \mathrm{nm}^{-1}$ with five higher orders indicate a lamellar period of $L \approx 9$ nm with long-range spatial order. This lamellar period is somewhat smaller than in the bulk (10.7 nm). The large intensity of the third order is due to superposition with the first-order Bragg peak from the smectic layering of about 3 nm parallel to the substrate. This indicates a rather special lamellar morphology in the diblock film, with both smectic and amorphous layers parallel to the substrate. The total thickness of 36 nm corresponds to four lamellar blocks. Fits to the reflectivity data indicate that the density profile through the film can be described by 12 layers of thickness of about 3 nm (±15%) while the interfacial roughness varies between 0.5 and 1 nm. Moreover, the density profile decreases monotonically from the substrate to the air/film interface leading to unrealistically low values for most of the layers. We are aware of one other report of parallel alignment of smectic layers and block lamellae [49], in which case it was attributed to peculiarities of the Sm-C* phase involved.

More insight about the diblock film structure is provided by the AFM data of Fig. 6. One can see terraces with a thickness of about 9 nm, the area of which decreases monotonically from the substrate to the air. Hence, the AFM image confirms the presence of lamellae parallel to the substrate. The decrease in area of the terraces on top of each other is consistent with the

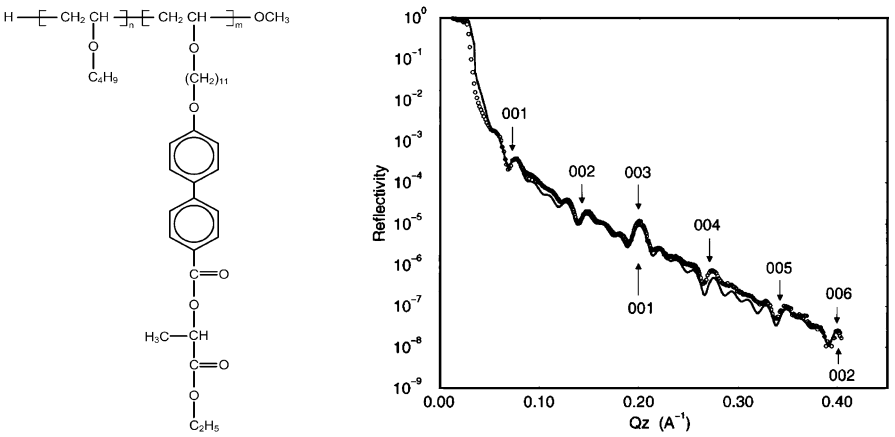

Fig. 5 **a** Structure of PIBVE-PLC. **b** X-ray reflectivity of a 36 nm thick film after annealing in the Sm-A phase at $T = 63\ ^\circ\mathrm{C}$ (*circles*) with possible fitting curve (*solid line*) as discussed in the text. The Bragg positions of the diblock periodicity (*above the curve*) and of the smectic spacing (*below the curve*) are indicated [48]

monotonic decreasing density of the slabs in the XR model. It suggests that the organization of the lamellar structure starts from the substrate level. Reasonable fits of the XR data can be obtained by averaging the reflectivity of four different films of thickness of 1 to 4 lamellae, respectively, and realistic densities. We further notice in Fig. 6 instabilities during the microphase separation: the AFM picture shows intermediate layers of thickness of about 3 nm between adjacent terraces. These layers are dewetting the underneath terrace as indicated by their irregular contours. In fact, during the phase segregation process, islands and depressions of this thickness are successively formed, which are unstable at the air/film interface, leaving a few stable terraces of approximately 9 nm.

In the present film system the lamellar period must be composed of a smectic block of about 6 nm, and an amorphous block of approximately 3 nm, in order to be consistent with the bulk volume fractions of the blocks. Generally, such a parallel lamellar structure will be configurationally frustrated, because the smectic block size, as obtained by scaling the lamellar diblock period, may be incommensurate with the smectic periodicity [44]. However, for the present volume fractions, the smectic block size corresponds to twice the smectic periodicity. Several lamellar morphologies with block interfaces and smectic layers parallel are potentially possible. Various combinations of alternating amorphous blocks and an integral number of smectic layers can be obtained, with the mesogens oriented "up" and "down" with respect to the backbone. However, for neither of these cases, a lamellar period around 9 nm can be constructed. Moreover, such a situation leads to an unfavorable contact area between A and B components. Remember that the main segregation is due to the unfavorable χ_{AB} between the amorphous polymer

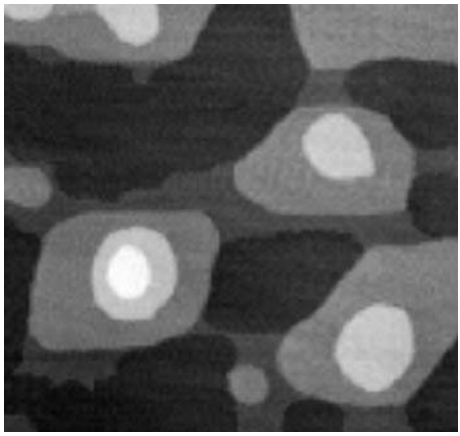

Fig. 6 AFM image of a dewetted PIBVE-PLC film ($10 \times 10\,\mu m^2$). The height difference between the terraces is about 9 nm. Dewetting layers of a thickness of about 3 nm can be seen adjacent to the terraces

A and the mesogenic units B and to $\chi_{A'B}$ between the backbone A′ and its side groups B. These considerations led to a radically different proposal for the mesogen packing within the smectic layers. The mesogenic units are assumed to be densely packed, all pointing to the same direction (Fig. 7b). Alternating with the smectic layers, the PIBVE block will form the second sublayer. As the side groups point to the same direction, the polymer A and backbone A′ face each other in a favorable way, because they are essentially of the same chemical composition and $\chi_{AA'} \approx 0$. In addition, phase segregation is ensured between the A, A′ components at one side and the B component at the other side. In this situation, the smectic and amorphous block sizes correspond to about 6 and 3 nm, respectively, in agreement with the lamellar period. It seems that, in contrast to the bulk and homopolymer situations, a unidirectional conformation of the mesogens is the only way that allows a combination of the phase-separated structure and the smectic LC/substrate preferential interactions.

The difference in stability between the bulk structure of Fig. 7a and the film structure of Fig. 7b can be rationalized in terms of the influence of the surface [48]. First, the free energy contributions of the smectic ordering in the bulk and in the film are different because of the dissimilar packing configurations of the mesogens. The interdigitated smectic ordering of Fig. 7a is the natural morphology and is expected be more favorable than that of Fig. 7b, which requires a relatively strong confinement of the mesogens. However, this may be outweighed by the contribution from the block-block transition layer that contributes in the bulk (see Fig. 7a) unfavorably to the free energy of mixing of the A and B components. In the proposed film structure this is replaced by favorable AA′ interactions. For the packing configuration of the amorphous block only minor changes are expected.

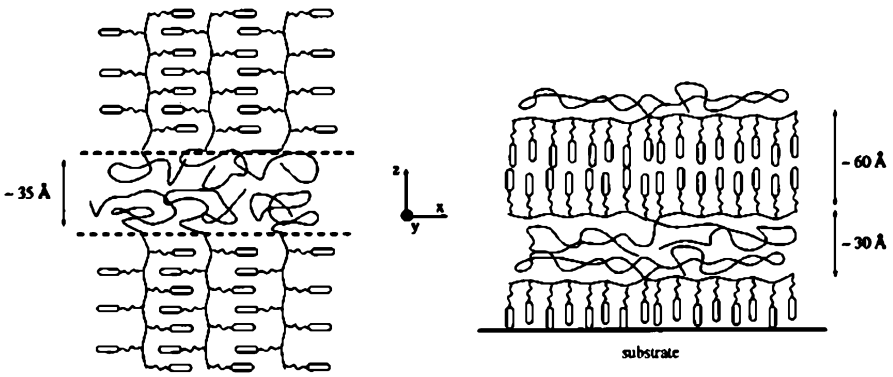

Fig. 7 Microscopic model of PIBVE-PLC for **a** the bulk orthogonal lamellar morphology and **b** the thin film parallel lamellar morphology

In conclusion the parallel lamellar structure of Fig. 7b seems to originate from the strong interaction between the mesogenic units and the substrate. The favorable internal diblock interactions will maintain the parallel lamellar structure, as long as the entropy cost due to the confinement of mesogens within the smectic layers is compensated for by the mesogens/substrate enthalpy bonus. The instability of the lamellar structure as observed in AFM (dewetting layers and terraces with decreasing area from the substrate to the air) indicates that this is not the case for all thicknesses. This point has not been investigated in further detail. Finally, we must conclude that though the situation of parallel block lamellae and smectic layers may be interesting from a physical point of view, it does not allow access to the layering in terms of nanostructuring. Unfortunately, samples with a probably useful cylindrical morphology were not available.

5
Example 3. Fluorinated Smectic/Amorphous Diblock Copolymer

Fluorinated polymers are of special interest because of the specific surface affinity of the fluorinated parts. This adds an extra element to the discussion so far. Coatings with controlled organization of the fluorinated parts are of interest as water/dirt repellent systems [50–53]. Fluorinated alkanes attached as side groups to a polymer can organize in smectic layers. Block copolymer ordering can be added as a third element to the smectic organization and the surface affinity of the fluorinated groups. In the example to be discussed [55], we move away from lamellar structures at about equal volume fractions and use the asymmetric compound PMMA-*b*-PF8H2A pictured in Fig. 8a (further properties in Table 1). Note that the backbone polymer is again rather similar (but not equal) to the amorphous polymer: in the A(A′B) picture we now expect $\chi_{AA'}$ to be small but not zero. Because of the strong difference with the fluorinated side chain we expect $\chi_{A'B} \approx \chi_{AB} \gg \chi_{AA'}$.

Small-angle X-ray scattering in the bulk shown in Fig. 8b indicates a hexagonal structure. Moreover, the two blocks are strongly microphase separated: $T_{ODT} > 300\,^{\circ}C$. Upon cooling, a Sm-A phase appears within the fluorinated block below about 85 °C. The mesogens organize in double layers with a period $d \approx 3.3$ nm. The X-ray peaks corresponding to the microphase separated structure are not affected by the additional LC ordering. Single domain samples reveal that the smectic layers are perpendicular to the cylindrical block interfaces, in agreement with results for other fluorinated smectic/amorphous block copolymers [52, 56, 57]. While this situation is common from lamellar structures, it is not obvious for the other morphologies. In fact several cases have been reported of smectic layers parallel to the cylindrical block interfaces [43, 57].

Thin films of PMMA-*b*-PF8H2A were investigated with XR [55]. A typical result shown in Fig. 9a indicates rather rough interfaces (the Kiessig fringes

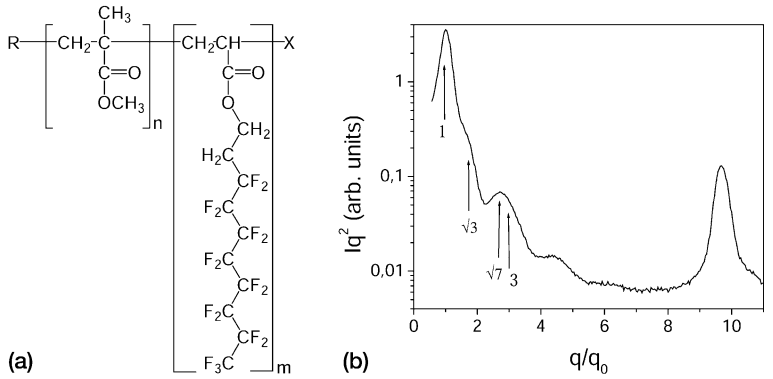

Fig. 8 **a** Structure of PMMA-*b*-PF8H2A; $n = 80$, $m = 74$. **b** Small-angle X-ray scattering in the bulk indicating hexagonal ordering with $L = 31.5$ nm and smectic layering with $d = 3.3$ nm

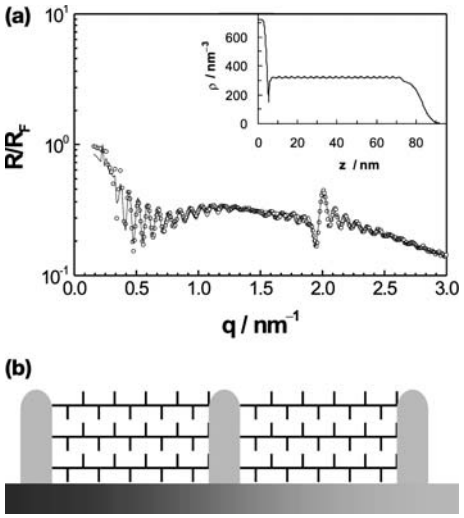

Fig. 9 **a** XR divided by the Fresnel reflectivity R_F and corresponding fit (*full line*) of a 82 nm film of PMMA-*b*-PF8H2A. **b** Associated model [55]

are not very well developed) and a smectic peak around $q = 2.01$ nm^{-1}. The corresponding spacing of 3.2 nm is very close to the bulk smectic spacing of 3.3 nm. This indicates that the smectic layers are aligned parallel to the substrate with the fluorinated chains anchoring homeotropically to the substrate. The best fit to the XR data indicates that the density profile through the film is composed of 21 smectic layers with a spacing of 3.2 nm sandwiched between different bottom and top layers (see inset of Fig. 9a). From this information we arrive at the preliminary model of Fig. 9b. Gronski and co-workers obtained somewhat similar results [34]. The latter authors describe in addition

situations of random as well as regular positioning of the cylinders. Ordered arrays of perpendicular cylinders were recently also reported in thin films of a hybrid smectic/amorphous block copolymer with azobenzene mesogenic side-groups [59]. All these results indicate stabilization of a perpendicular orientation of the cylinders by smectic layering parallel to the substrate.

In general, for "classical" amorphous block copolymers one can expect cylinders perpendicular to the substrate if the possible gain in surface energy from preferential absorption of one of the blocks is more than compensated by the free energy change associated with the elastic distortions of the chain. This point was nicely demonstrated in the work of Russell and coworkers [60], who realized films with a perpendicular orientation of cylinders by making the substrate neutral to both blocks via coating with a random copolymer. Alternatively, perpendicular orientation of cylinders has been reached by applying an electric field [61] as well as by slow evaporation of the solvent after spin-coating [62, 63].

Figure 10a shows an AFM phase image of an annealed film at room temperature. Cylindrical PMMA domains (dark areas) can be seen, oriented normal to the surface and covering the whole surface of the film. The average diameter of the PMMA cylinders is about 18 nm and the average center-to-center distance between the cylindrical domains is approximately 35 nm. From the images there seems to be no long-range lateral order of the cylindrical domains. More information about the average in-plane ordering was obtained by grazing-incidence X-ray diffraction. In GIXD the X-ray beam shines on a surface at a small glancing angle α. If α is smaller than the critical angle α_c, total reflection occurs; now only an evanescent wave penetrates into the film. Using this wave as the "incident" beam, two-dimensional in-plane X-ray diffraction can be performed. The penetration depth of the X-rays depends on α and can be set to probe the full film. Hence, potentially GIXD allows us to quantify the internal structure of the blocks and to validate any model. In films of PMMA-*b*-PF8H2A a broad peak was found, corresponding to the liquid in-plane order of the fluorinated smectic block at an average distance of about 0.5 nm. This confirms the parallel orientation of the smectic layers with respect to the substrate as seen in XR. Any block structure would be at small angles and can only be observed with grazing-incidence small-angle X-ray scattering (GISAXS), the result of which is shown in Fig. 10b. The peak at $q = 0.207\ \mathrm{nm}^{-1}$ corresponds to an average in-plane periodicity of 30.3 nm. This is very close to the interdomain period in the bulk (31 nm) and proves that the cylindrical domains are not only oriented normal to the air interface but span the entire film thickness. The peak can be well fitted by a Lorentzian function with a correlation length of about 40 nm (short-range liquid-like ordering).

In conclusion, AFM and grazing-incidence X-ray scattering essentially confirm the model of Fig. 9b. The cylindrical PMMA domains stand normal to the substrate and span the entire film. They are embedded in a matrix

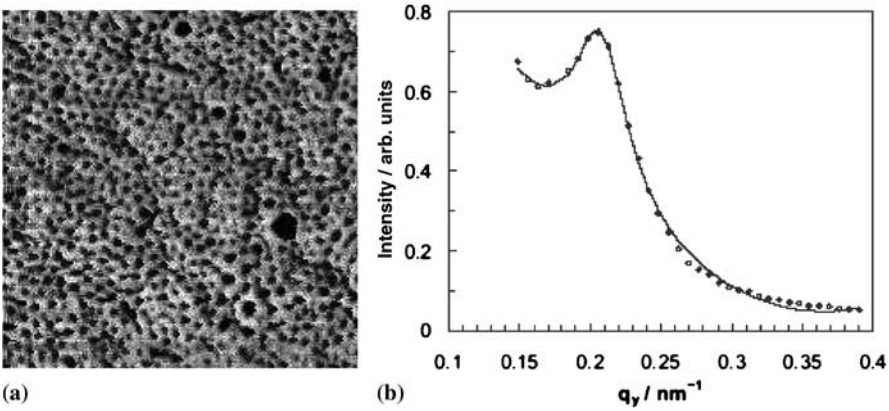

Fig. 10 Evidence for perpendicular cylinders in an annealed PMMA-*b*-PF8H2A film at room temperature. **a** AFM phase image in the tapping mode ($1 \times 1\ \mu m^2$). **b** GISAXS curve fitted to Lorentzian (*full line*)

of the PF8H2A phase with the side chains forming smectic bilayers parallel to the substrate. The structure can be understood in terms of the combined effect of the microphase separation, the smectic ordering and the orientational wettability of the side chains. At the air-film interface the fluorinated side chains orient toward air in order to lower the surface energy [64]. This would cause the smectic layers to orient parallel to the substrate. However, the smectic layers also tend to orient perpendicular to the microdomain interfaces in order to minimize the contact area between the two polymer blocks. Hence, to simultaneously maintain these preferential interactions the smectic layers and the cylindrical domains orient parallel and perpendicular to the substrate, respectively. Though the film has been annealed above the smectic-isotropic transition, evidently the essential elements leading to the smectic layering are already present locally at the interfaces.

6 Conclusions and Outlook

There is little doubt that supramolecular materials built from highly regular molecular nanostructures can possess interesting visco-elastic or electrical properties and may sensitively respond to various external fields (sensors). Furthermore, their nanostructured surfaces can exhibit highly selective interactions with molecules in the environment (biosensors). Nevertheless, we are only at the edge of coming to realistic applications. Controlled nanopatterning is a prerequisite for further progress. For various applications (nano-pore size filters, generation of a two-dimensional electric potential, medium for electrophoresis of DNA) simple periodic patterning is sufficient. Compet-

ing length scales provide a valuable tool to obtain and control the required nanopatterns.

In this review we have shown that thin films with periodic arrays of lamellae or cylinders perpendicular to a substrate can be nicely stabilized using the "tandem" interactions in hybrid smectic LC/amorphous block copolymers. Advantages over other methods [60–63] are: (i) absence of chemical treatment of the substrate; (ii) minimum number of steps in which the final result is accomplished; and (iii) robustness against annealing (within the smectic temperature range) because the structures are in thermodynamic equilibrium. Starting from a lamellar block morphology, the smectic LC layering stabilizes perpendicular block lamellae. However, control of the azimuthal orientation remains difficult so far [44, 46]. From this point of view stabilizing a cylindrical block morphology perpendicular to the substrate by parallel smectic layering is easier. A major recent achievement is stabilization by smectic layering of long-range order of the cylinders over large areas [59]. Possibilities of chemical variation of the liquid-crystal block have so far hardly been explored. Selective etching allows obtaining a variety of structures, in the case of cylinders either nano-holes or nano-pillars [65]. Applications of such possibilities are potentially numerous, but still require further investigations. In the mean time the physics involved is fascinating.

Acknowledgements The authors want to thank the members of the EU-POLYNANO network and Denitza Lambreva (AMOLF, Amsterdam) for fruitful discussions and cooperation over the past years. Gerard Wong and Daniel Sentenac are acknowledged for their contributions in the early stages. This work is supported in part by the European Community's Human Potential Programme under contract HPRN-CT-1999-00151 (POLYNANO) and is part of the research program of the "Stichting voor Fundamenteel Onderzoek der Materie (FOM)", which is financially supported by the "Nederlandse Organisatie voor Wetenschappelijk Onderzoek (NWO)". Y. Séréro and M. Al-Hussein acknowledge financial support provided through POLYNANO.

References

1. Muthukumar M, Ober CK, Thomas EL (1997) Science 277:1225
2. Park C, Thomas EL (2003) Adv Mater 15:585
3. Park M, Harrison C, Chaikin PM, Register RA, Adamson DH (1997) Science 276:1401
4. Rockford L, Mochrie SG, Russell TP (2001) Macromolecules 34:1487
5. Schaffer E, Thurn-Albrecht T, Russell TP, Steiner U (2000) Nature 403:874
6. Yang XM, Peters RD, Nealey PF, Solak HS, Cerrina F (2000) Macromolecules 33:9575
7. Bates FS, Fredrickson GH (1990) Annu Rev Phys Chem 41:525
8. Bates FS, Fredrickson GH (1999) Physics Today February:32
9. Hamley IW (1998) The Physics of Block Copolymers. Oxford University Press, New York
10. Russell TP, Coulon G, Deline VR, Miller DC (1989) Macromolecules 22:4600
11. Russell TP (1990) Mater Sci Rep 5:171
12. Coulon G, Russell TP, Deline VR, Green PF (1989) Macromolecules 22:2581

13. Coulon G, Collin B, Aussere D, Chatenay D, Russell TP (1990) J Phys (Paris) 51:2801
14. McArdle CB (ed) (1989) Side Chain Liquid Crystalline Polymers. Blackie, Glasgow
15. Plate NA (ed) (1993) Liquid-Crystal Polymers. Plenum, New York
16. Hardouin F, Mery S, Achard MF, Noirez L, Keller P (1991) J Phys (Paris) Lett 1:511
17. Pragliola S, Ober CK, Mather PT, Jeon HG (1999) Macrom Chem Phys 200:2338
18. Zhou QF, Zhu XL, Wen ZQ (1989) Macromolecules 22:491
19. Guillon D, Poeti G, Skoulios A, Fanelli E (1983) J Phys (Paris) Lett 44:L-491
20. Diele S, Oelsner S, Kuschel F, Hisgen B, Ringsdorf H, Zentel R (1987) Macrom Chem Phys 188:1993
21. Al-Hussein M, de Jeu WH, Vranichar L, Pispas S, Hajichristidis N, Itoh T, Watanabe J (2004) Macromolecules 67:6401
22. Chiellini E, Galli G, Angeloni AS, Laus M (1994) Trends Polym Sci 2:244
23. Walther M, Finkelmann H (1996) Progr Polym Sci 21:951
24. Poser S, Fischer H, Arnold M (1998) Prog Polym Sci 23:1337
25. Kato T (2002) Science 295:2414
26. Lee M, Cho B, Zin W (2001) Chem Rev 101:3669
27. Adams J, Gronski W (1989) Macrom Chem Rapid Commun 10:553
28. Bohnert R, Finkelmann H (1994) Macrom Chem Phys 195:689
29. Fischer H, Poser S, Arnold M, Frank W (1994) Macromolecules 27:7133
30. Yamada M, Uguchi T, Hirao A, Nakahama S, Watanabe J (1995) Macromolecules 28:50
31. Mao G, Wang J, Clingman SR, Ober CK, Chen JT, Thomas EL (1997) Macromolecules 30:2556
32. Sanger J, Gronski W, Maas S, Stuhn B, Heck B (1997) Macromolecules 30:6783
33. Galli G, Chiellini E, Laus M, Ferri D, Wolff D (1997) Macromolecules 30:3417
34. Figueiredo P, Geppert S, Brandsch R, Bar G, Thomann R, Spontak RJ, Gronski W, Samlenski R, Mueller-Buschbaun P (2001) Macromolecules 34:171
35. Anthamatten M, Hammond PT (2001) Macromolecules 34:8574
36. Ansari IA, Castelletto V, Mykhaylyk T, Hamley IW, Lu ZB, Itoh Y, Imrie CT (2003) Macromolecules 36:8898
37. Jérome B, Commandeur J, de Jeu WH (1997) Liq Cryst 22:685
38. Ikkala O, ten Brinke G (2002) Science 295:2407
39. Ruokolainen J, Makinen R, Torkkeli M, Makela T, Serimaa R, ten Brinke G, Ikkala O (1998) Science 280:557
40. Tolan M (1999) X-ray Scattering from Soft-Matter Thin Films. Springer, Heidelberg
41. Als-Nielsen J, Jacquemain D, Kjaer K, Leveiller F, Lahav M, Leiserowitz L (1994) Phys Rep 246:251
42. Madsen A, Konovalov O, Robert A, Gruebel G (2001) Phys Rev E 64:61406
43. Fischer H, Poser S, Arnold M (1995) Liq Cryst 18:503
44. Wong GCL, Commandeur J, Fischer H, de Jeu WH (1996) Phys Rev Lett 26:5221
45. Niederhauser TL, Jiang G, Lua Y-Y, Dorff MJ, Woolley AT, Asplund MC, Berges DA, Lindford MR (2001) Langmuir 17:5889
46. Sivaniah E, Hayashi Y, Iino M, Hashimoto T, Fukunaga K (2003) Macromolecules 36:5894
47. Omenat A, Hikmet RAM, Lub J, van der Sluis P (1996) Macromolecules 29:6730
48. Sentenac D, Demirel A, Lub J, de Jeu WH (1999) Macromolecules 32:3235
49. Zheng W-Y, Albalak RJ, Hammond PT (1998) Macromolecules 31:2686
50. Krupers M, Slangen P-J, Moeller M (1998) Macromolecules 31:2552
51. Genzer J, Sivaniah E, Kramer EJ, Wang J, Korner H, Xiang M, Char K, Ober CK, Sambasivan S, Fischer DA (2000) Macromolecules 33:1882
52. Li X, Ruzzi L, Chiellini E, Galli G, Ober CK, Hexemer A, Kramer EJ, Fischer DA (2002) Macromolecules 35:8078

53. Schmidt DL, Coburn CE, DeKoven BM, Potter GE, Meyers GF, Fisher DA (1994) Nature 368:39
54. Krupers M, Moeller M (1997) Macrom Chem Phys 198:2163
55. Al-Hussein M, Séréro Y, Konovalov O, Mourran A, Moeller M, de Jeu WH (2005) Macromolecules 38 (in press)
56. Osuji C, Zhang Y, Mao G, Ober CK, Thomas EL (1999) Macromolecules 32:7703
57. Wang J, Mao G, Ober CK, Kramer EJ (1997) Macromolecules 30:1906
58. Anthamatten M, Hammond PT (1999) 32:8066
59. Iyoda T, Kamata K, Watanabe K, Watanabe R, Yoshida H (2004) E-polymers, Macro-04 (Paris) Session 221
60. Mansky P, Liu Y, Huang E, Russell TP, Hawker C (1997) Science 275:1458
61. Thurn-Albrecht T, DeRouchey J, Russell TP, Jaeger HM (2000) Macromolecules 33:3250
62. Lin ZQ, Kim DH, Wu XD, Boosahda L, Stone D, LaRose L, Russell TP (2002) Adv Mater 14:1373
63. Kim SH, Misner MJ, Xu T, Kimura M, Russell TP (2004) Adv Mater 16:226
64. Wu SH (1982) Polymer Interfaces and Adhesion. Marcel Dekker, New York
65. Thurn-Albrecht T, Steiner R, DeRouchey J, Stafford CM, Huang E, Bal M, Tuominen M, Hawker CJ, Russell TP (2000) Adv Mater 12:787